

Naval Surface Warfare Center Carderock Division

West Bethesda, MD 20817-5700

NSWCCD-TR-61 — 1998/30 Nov 1998

Survivability, Structures, and Materials Directorate
Technical Report

An Experimental Evaluation of the Fatigue Behavior of AH36 Weld-Repaired Deck Sockets in a Simulated Marine Atmosphere

by

Michelle A. Gaudett
X. Jie Zhang

19990923 017



Approved for public release; distribution is unlimited.

DTIC QUALITY INSPECTED 4

REPORT DOCUMENTATION PAGE

Form Approved
OMB No. 0704-0188

1. AGENCY USE ONLY (Leave blank)		2. REPORT DATE November 1998	3. REPORT TYPE AND DATES COVERED Research and Development Report	
4. TITLE AND SUBTITLE An Experimental Evaluation of the Fatigue Behavior of AH36 Weld-Repaired Deck Sockets in a Simulated Marine Atmosphere			5. FUNDING NUMBERS 1-2200-806 1-2200-807 1-2200-847	
6. AUTHOR(S) Dr. Michelle A. Gaudett Dr. X. Jie Zhang				
7. PERFORMING ORGANIZATION NAME(S) AND ADDRESS(ES) Code 6140, Carderock Division Naval Surface Warfare Center 9500 MacArthur Blvd. West Bethesda, MD 20817-5700			8. PERFORMING ORGANIZATION REPORT NUMBER NSWCCD-TR-61-1998/30	
9. SPONSORING/MONITORING AGENCY NAME(S) AND ADDRESS(ES) Strategic Sealift Program Office Naval Sea Systems Command Arlington, VA 22242-5160			10. SPONSORING/MONITORING AGENCY REPORT NUMBER	
11. SUPPLEMENTARY NOTES				
12a. DISTRIBUTION/AVAILABILITY STATEMENT Approved for public release; distribution is unlimited.			12b. DISTRIBUTION CODE Statement A	
13. ABSTRACT (Maximum 200 words) Fatigue testing of specimens removed from weld-repaired deck sockets on the fast sealift ship was conducted to satisfy two objectives. The primary objective was to determine the shift in fatigue initiation behavior due to an intermittent salt spray environment. The secondary objective was to validate the fatigue initiation design curves used in the fatigue analysis of the ship deck structure. No effect of a salt spray schedule was observed within the low stress, high cycle fatigue regime examined ($\Delta\sigma = 0.6\sigma_y$ to $1.0\sigma_y$, $N_f = 2 \times 10^5$ to 10^7 cycles). However, an effect of the salt spray schedule was observed within the high stress, low cycle regime ($\Delta\sigma = 1.2\sigma_y$ to $1.7\sigma_y$, $N_f = 1.5 \times 10^4$ to 4×10^5 cycles) and an approximate maximum fatigue reduction factor ($\Delta\sigma_{air}/\Delta\sigma_{salt\ spray}$) of 1.4 was observed. Comparison of the fatigue data obtained in this study with the design fatigue curves is consistent with the known effect of specimen size on fatigue behavior. This work verified that the design fatigue curves obtained from large welded specimens represents a lower bound for the fatigue behavior of weld-repaired deck sockets tested in air, as well as under a corrosive salt spray schedule.				
14. SUBJECT TERMS fatigue initiation, corrosion fatigue, ABS AH36 steel, weld, fatigue design data, AASHTO			15. NUMBER OF PAGES 12	
			16. PRICE CODE	
17. SECURITY CLASSIFICATION OF REPORT Unclassified	18. SECURITY CLASSIFICATION OF THIS PAGE Unclassified	19. SECURITY CLASSIFICATION OF ABSTRACT Unclassified	20. LIMITATION OF ABSTRACT Unclassified	

TABLE OF CONTENTS

LIST OF FIGURES	II
LIST OF TABLES	II
ABSTRACT.....	III
EXECUTIVE SUMMARY	IV
ACKNOWLEDGEMENTS	IV
INTRODUCTION.....	1
MATERIALS AND EXPERIMENTAL PROCEDURE.....	1
RESULTS	4
Fatigue Testing	4
Specimen Examination	5
DISCUSSION	10
Effects of the Salt Spray Schedule on Fatigue Life.....	10
Comparison of Results to AASHTO Curves.....	11
CONCLUSIONS	12
REFERENCES.....	12

LIST OF FIGURES

Figure 1 Orientation of test specimens removed from cloverleaf deck sockets.....	3
Figure 2 - Schematic of weld-repaired fatigue test specimen.	4
Figure 3 Alternating applied stress versus cycles to failure for weld-repaired AH36 deck sockets tested in three-point bending.	6
Figure 4 Maximum applied stress versus cycles to failure for weld-repaired AH36 deck sockets tested in three-point bending.	7
Figure 5 Optical macrograph of typical specimen tested in air showing fracture along weld and base metal interface.....	8
Figure 6 Scanning electron micrograph of specimen S7#1 near fatigue crack tip ($\Delta\sigma=90.4 \text{ ksi}=1.7\sigma_y$, $N_f=51,863$ cycles.).....	9
Figure 7 Scanning electron micrograph of specimen S6#2(1) near fatigue crack tip ($\Delta\sigma=30.4 \text{ ksi}=0.6\sigma_y$, $N_f=10,302,827$ cycles.).....	9

LIST OF TABLES

Table I Typical mechanical properties of AH36 steel used in deck sockets.....	2
Table II Salt spray/humidity schedule employed for accelerated corrosion testing..	3
Table III Fatigue results for weld-repaired AH36 deck sockets tested in laboratory air (R=0.1).....	6
Table IV Fatigue results for weld-repaired AH36 deck sockets tested under salt spray application (R=0.1).....	7
Table V Linear regression results of the fatigue life data using the equation $\log\Delta\sigma = m\log N + b$ or $\log\sigma_{\max} = m\log N + b$	8

ABSTRACT

Fatigue testing of specimens removed from weld-repaired deck sockets on the fast sealift ship was conducted to satisfy two objectives. The primary objective was to determine the shift in fatigue initiation behavior due to an intermittent salt spray environment. The secondary objective was to validate the fatigue initiation design curves used in the fatigue analysis of the ship deck structure. No effect of a salt spray schedule was observed within the low stress, high cycle fatigue regime examined ($\Delta\sigma = 0.6\sigma_y$ to $1.0\sigma_y$, $N_f = 2 \times 10^5$ to 10^7 cycles). However, an effect of the salt spray schedule was observed within the high stress, low cycle regime ($\Delta\sigma = 1.2\sigma_y$ to $1.7\sigma_y$, $N_f = 5 \times 10^4$ to 4×10^5 cycles) and an approximate maximum fatigue reduction factor ($\Delta\sigma_{\text{air}}/\Delta\sigma_{\text{salt spray}}$) of 1.4 was observed. Comparison of the fatigue data obtained in this study with the design fatigue curves is consistent with the known effect of specimen size on fatigue behavior. This work verified that the design fatigue curves obtained from large welded specimens represents a lower bound for the fatigue behavior of weld-repaired deck sockets tested in air, as well as under a corrosive salt spray schedule.

EXECUTIVE SUMMARY

The presence of numerous installed deck sockets containing weld-repaired cracks on the led to concern regarding the fatigue lives of the weld-repaired deck sockets on the fast sealift ships. This work was initiated to address this concern. The primary objective of this work is to evaluate the effect of the marine atmosphere on the fatigue life of a weld-repaired deck socket. A secondary objective of this experimental work was to validate the standard ambient environment S-N curves used in the fatigue life analyses. An attempt was made to understand the effect of specimen size on the measured fatigue lives by comparing results for the smaller deck socket specimens and the standard large scale specimens.

Specimens were removed from weld-repaired deck sockets and tested in three point bending under load control ($R=P_{\min}/P_{\max}=0.1$). A modified salt spray schedule was employed to assess the effect of a marine environment on fatigue initiation behavior. The ambient environment tests were conducted at 10 Hz, and the salt spray schedule tests were conducted at 1 Hz. The salt spray schedule resulted in significant corrosion of the deck socket surface.

No effect of a salt spray schedule was observed in the high cycle portion of the fatigue data ($\Delta\sigma = 0.6\sigma_y$ to $1.0\sigma_y$, $N_f = 2 \times 10^5$ to 10^7 cycles). However, an effect of the salt spray schedule was observed within the high stress, low cycle regime ($\Delta\sigma = 1.2\sigma_y$ to $1.7\sigma_y$, $N_f = 1.5 \times 10^4$ to 4×10^5 cycles) and an approximate maximum fatigue reduction factor ($\Delta\sigma_{\text{air}}/\Delta\sigma_{\text{salt spray}}$) of 1.4 was observed. Almost all the specimens failed along the weld/base metal interface. It appears that the surface corrosion did not have a large effect on fatigue initiation at long fatigue lives due to the dominating effect of the stress concentration at the weld/base metal interface. At short fatigue lives it appears that the high level of local plastic deformation (due to high applied stresses) enhanced the corrosion rate and localized corrosion at the weld/base metal interface, resulting in a reduced fatigue life compared to the air tests. No significant differences in the fracture modes of the specimens tested in air compared to the salt spray environment were observed.

Comparison of the fatigue data obtained in this study with the design fatigue curves is consistent with the known effect of specimen size on fatigue behavior. This work verified that the standard design fatigue curves obtained from large welded specimens represents a lower bound for the fatigue behavior of weld-repaired deck sockets tested in air, as well as under a corrosive salt spray schedule.

ACKNOWLEDGEMENTS

This work was sponsored by the Strategic Sealift Program Office (K. Lynaugh) and PMS385 (J. Sandison). The work was performed within the Fatigue and Fracture Branch (Code 614) of the Naval Surface Warfare Center, Carderock Division, under the supervision of T. Montemarano, Head, Fatigue and Fracture Branch. The finite element analysis described in the report was performed by Gerard Mercier (Code 614). The technical assistance of Erick Satchell with the fatigue testing is gratefully acknowledged (Code 614).

INTRODUCTION

Cracking of Types 518E and 518F AH36 steel cloverleaf deck sockets was observed after installation in fast sealift ships in various stages of construction. Cracking initiated from the tip of the cloverleaf pattern in all cases. A subsequent failure analysis identified the cause of cracking and recommended procedures that would eliminate any further crack initiation in the newly produced deck sockets¹. The numerous installed deck sockets containing cracks were weld-repaired, which led to concern regarding the fatigue lives of the weld-repaired deck sockets.

To address this concern, a detailed fatigue analysis of the deck sockets had been conducted which quantified the extent and magnitude of calculated fatigue failures for a 40 year ship life. The low cycle fatigue initiation behavior of various structural steels and welds were obtained from standard S-N curves compiled for various structural details (AASHTO²). This analysis shows that in certain ship locations, the projected weld-repaired deck socket fatigue life is only 5 years.

The objective of this experimental work is two-fold. The standard AASHTO S-N curves used in the fatigue analyses of the ship deck structure does not take into account any environmental effects. Since the deck sockets are exposed to a moist marine atmosphere, are periodically wetted by seawater and show considerable corrosion on unpainted surfaces, a concern was raised regarding the effects of corrosion on the AASHTO S-N curves. Therefore, a primary objective was to evaluate the effect of the marine atmosphere on the fatigue life of a weld-repaired deck socket.

A secondary objective of this experimental work was to validate the neutral environment AASHTO S-N curves used in the fatigue life analyses. An attempt was made to understand the effect of specimen size on the measured fatigue lives by comparing results for the smaller deck socket specimens and the large scale AASHTO specimens.

MATERIALS AND EXPERIMENTAL PROCEDURE

Eight AH36 deck sockets (S1, S3-S9) were provided to NSWCCD for test specimens. Measured mechanical properties of the base metal are listed in Table I. Weld repairs were performed at each intact lobe of the cloverleaf (some lobes had been sectioned for previous tests). A through-thickness V-groove that extended from the socket lobe towards the circumferential weld (~1.5-in. in length, $30^{\circ}+5^{\circ}/-0^{\circ}$ bevel angle, a 0.0625 ± 0.03125 -in. root face and a 0.0625 ± 0.03125 -in. root opening) was ground into each lobe (see Fig. 1) and subsequently repaired. A ceramic backing was used to control the backing weld contour. The area to be welded was pre-heated to 150°F and welding progressed from the circumferential weld towards the center of the deck socket. Filler metal ER70S-2 or ER70S-3 was employed.

The specimens were machined from the weld-repaired deck sockets as shown in Fig. 1. The weld face and backing weld face were ground flush with the deck socket thickness. The concave surface of the deck socket lobe was *not* ground and was tested in the as-welded condition (see Fig. 2). The configuration of the specimens simulates as closely as possible the loading orientation of the deck sockets due to actual ship deck stresses. The specimens were tested in three-point bending as shown in Fig. 2. An R-ratio (P_{min}/P_{max}) of 0.1 was selected for two reasons: (1) x-ray diffraction measurements indicate the possibility of residual tensile stresses in the deck socket that will result in tension-tension fatigue when the alternating ship deck stresses are superimposed and (2) $R > 0$ is a more severe case than $R < 0$ for a constant cyclic stress amplitude³. Testing was performed in load control at a frequency of 10 Hz under neutral conditions, and 0.1 Hz under intermittent salt spray conditions.

Table I Typical mechanical properties of AH36 steel used in deck sockets.

0.2% Yield Strength (ksi)	Ultimate Tensile Strength (ksi)	Elongation (%)	Reduction in Area (%)	Brinell Hardness (HB)
52.7	76	29	73	158

The number of cycles required to obtain a crack of a finite length was recorded, rather than complete separation of the specimen. It was verified that for the applied stresses employed in these tests, the time for growth from visible crack initiation to a crack length of ~0.375-in. was negligible compared to the total test time. Using this crack length to indicate fatigue failure enabled more efficient use of test time. The displacement limits on the test machine were set to trigger a machine shutdown when the ~0.375-in. crack length created enough specimen deflection. These conditions enabled uninterrupted testing. After failure the specimens were sprayed with an acrylic coating to preserve the fracture surfaces.

Studies have been conducted to evaluate the fatigue behavior of steels that are fully immersed in chloride solutions. It was observed that for a variety of steels and strength levels ($\sigma_y = 41-197$ ksi), endurance limits were reduced to similar low values regardless of the endurance limits in air⁴. The deck sockets are not fully immersed in service. However, corrosion of unpainted surfaces is observed due to the marine environment and can have an effect on fatigue life. Therefore, rather than fully immersing the test specimens, a schedule of salt spray and humidity exposure was employed.

The schedule was based on a General Motors Engineering Standard that describes an accelerated corrosion laboratory test method to evaluate automotive cosmetic corrosion. The schedule is shown in Table II. The salt spray solution consisted of a 5 wt. % NaCl solution mixed in accordance with ASTM B117⁵. The humidity chamber consisted of a sectioned Nalgene bottle into which the welded notch of the specimen was inserted and sealed. The bottle was left open during the salt spray portion of the schedule, allowing the specimen to dry in an ambient environment between each spray. Saturated towels were inserted and the bottle closed to maintain 95% humidity overnight and on weekends. The specimen was cyclically loaded throughout the entire schedule.

Table II Salt spray/humidity schedule employed for accelerated corrosion testing.

Time	Event
1100-1500	Salt spray application every 0.5 h
1500-0700	Humidity environment
0700-1100	Ambient environment
Weekends	Humidity environment

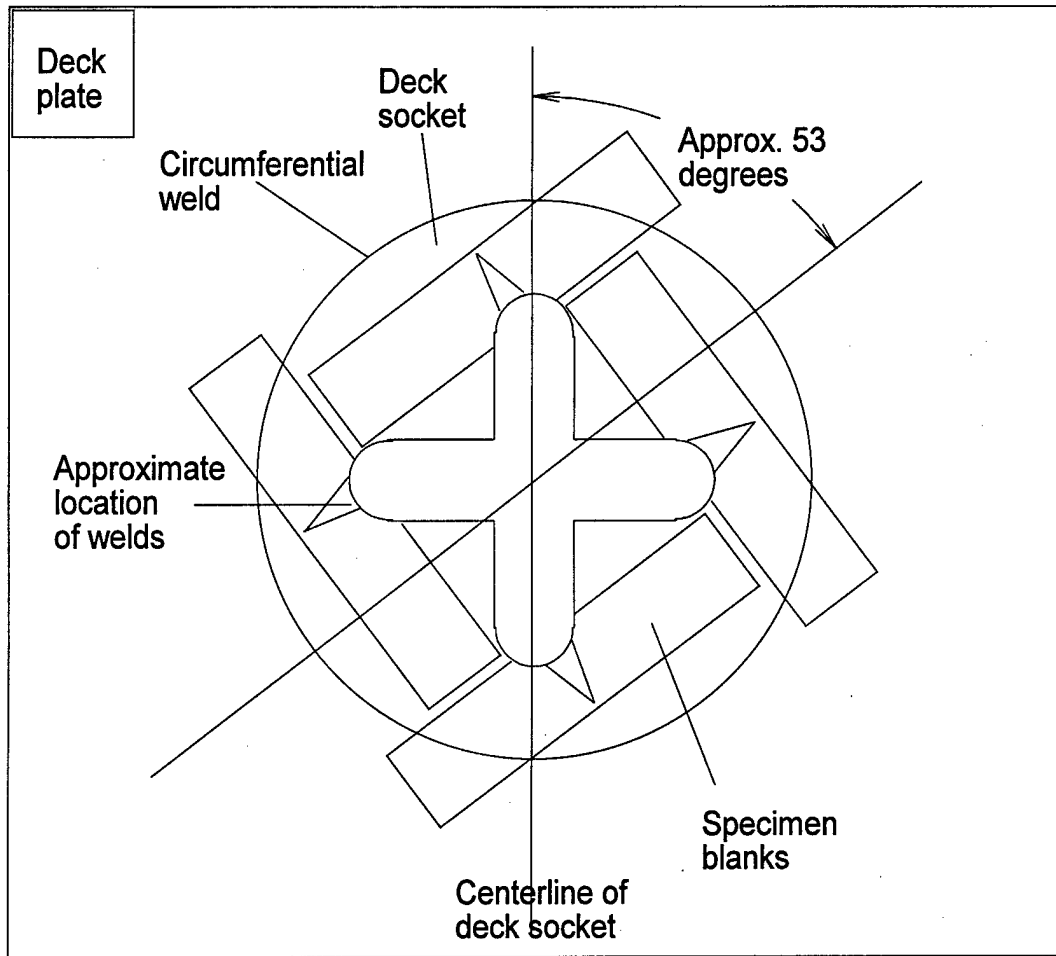


Figure 1 Orientation of test specimens removed from cloverleaf deck sockets.

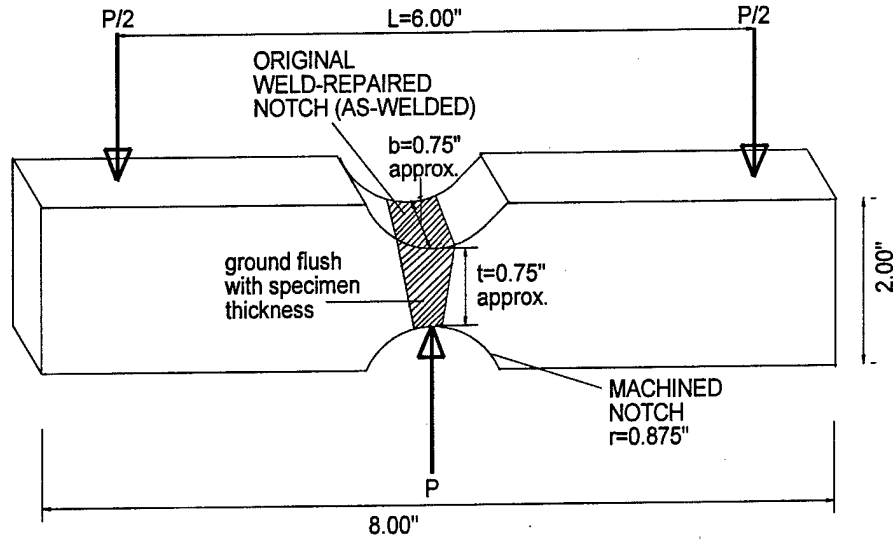


Figure 2 - Schematic of weld-repaired fatigue test specimen.

RESULTS

Fatigue Testing

The local applied stress range ($\Delta\sigma$, peak-to-peak) at the welded notch surface was calculated from the applied load range (ΔP) using the following equation:

$$\Delta\sigma = \frac{k_t 3\Delta PL}{2bt^2} \quad (1)$$

where k_t is the stress concentration factor of the weld-repaired notch (which does not take into account the as-welded surface), L is the distance between the two loading points (loading span), b is the specimen thickness (equal to ~0.75-in., the deck plate thickness) and t is the transverse specimen height (see Fig. 2).

A value for k_t was obtained from a three dimensional finite element analysis of the asymmetrical specimen. A 3-dimensional 0.75-in. thick mesh containing approximately 12,000 20-noded brick elements was constructed. Three-point bending was simulated by applying a force of 1500-lbf to the center of the machined notch. Nodes along the bottom edge were constrained in the vertical direction. Elastic properties with values of 30,000 ksi for the modulus and 0.3 for Poisson's ratio were used.

From this analysis a k_t value of 1.2 was obtained and employed to calculate $\Delta\sigma$. This value of k_t corresponds to the machined surface of the notch and does not take into account the as-welded surface. This value is in good agreement with a k_t value obtained from tabulated values for a notched plate with a minimum section of 0.75-in., notched

with semicircular grooves 0.625-in in depth and a radius of 0.875-in., loaded in bending ($k_t \approx 1.3$)⁶.

Results of the fatigue testing are shown in Tables III and IV and Figs. 3 and 4. Linear regressions of the $\log \Delta \sigma$ versus $\log N$ data were performed and are shown in Table V. The linear regression of the salt spray data includes data for failed specimens only.

Specimen Examination

All of the specimens, with the exception of two (S4#2 and S5#1), showed fatigue initiation and propagation in or near the fusion zone (i.e., at the weld/basemetal interface). Fig. 5 shows a macrograph of a typical (fully fractured) specimen viewed parallel to direction "t" in Fig. 2, looking down on the concave surface of the notch. It appears that the irregular surface geometry at the weld/base metal interface in the vicinity of the maximum stress served as a stress concentrator. In addition, since the weld material is harder than the base metal, one can surmise that the plastic deformation becomes localized within the softer base metal, becoming the preferred path for fatigue fracture.

A metallographic section of specimen S8#2 ($\Delta \sigma = 49 \text{ ksi} = 0.9 \sigma_y$) perpendicular to the fracture surface and parallel with the primary crack growth direction (and welding direction) was obtained. It appears that the primary fracture surface was contained within the base metal and initiated in a coarse grained heat-affected zone.

Selected specimens were cooled to liquid nitrogen temperatures and fully fractured subsequent to the fatigue testing described above. The two specimens that showed fatigue initiation and propagation within the weld were examined (S4#2 and S5#1). S5#1 possessed a lack of penetration or fusion defect (0.375-in. in depth) near the root of the weld that appeared to initiate fracture within the weld in this specimen. S4#2 showed multiple fatigue crack initiation, one along the fusion zone and one at a large lack of fusion defect near the root of the weld (similar to specimen S5#1).

The fracture surfaces of selected specimens are shown in Figs 6 and 7. Specimen S7#1 tested at $\Delta \sigma = 90 \text{ ksi} = 1.7 \sigma_y$ and specimen S6#2(1) tested at $\Delta \sigma = 30 \text{ ksi} = 0.6 \sigma_y$ were compared. The fracture mode showed a typical fatigue fracture morphology. The specimen tested at high stress (Fig. 6) showed more sharply defined and largely spaced

Table III Fatigue results for weld-repaired AH36 deck sockets tested in laboratory air (R=0.1).

Specimen No.	$\Delta\sigma$ (ksi)	σ_{max} (ksi)	Cycles to failure (N_f)
S6#1 (1)	29.5	32.9	1,797,643
S6#2 (1)	27.3	30.3	10,302,827
S5#2	40.3	44.8	1,503,454
S1#1	44.9	53.8	370,687
S9#2	63.5	75.2	430,710
S4#2	51.8	57.5	390,963
S1#2	59.5	69.9	231,035
S7#1	90.4	102.9	51,863
S8#1*	51.8	60.1	789,386

*696718 cycles in tension, rest in bending

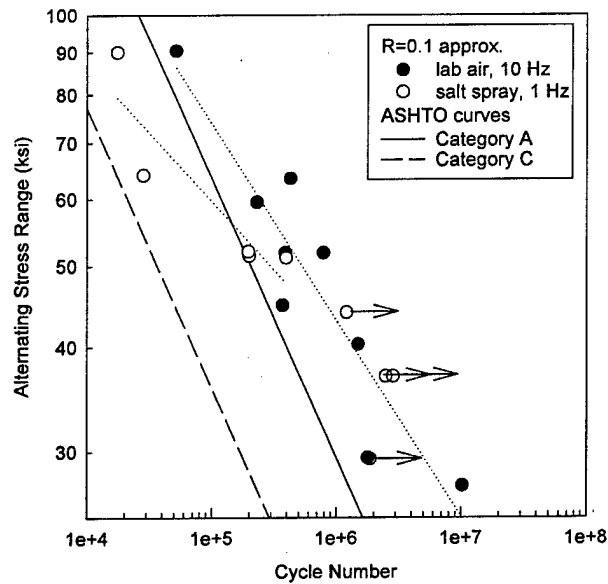


Figure 3 Alternating applied stress versus cycles to failure for weld-repaired AH36 deck sockets tested in three-point bending.

Table IV Fatigue results for weld-repaired AH36 deck sockets tested under salt spray application (R=0.1).

Specimen No.	$\Delta\sigma$ (ksi)	σ_{max} (ksi)	Cycle number
S4#1*	29.4	32.7	1,871,711
S3#1*	36.9	41.0	2,853,623
S9#4*	36.9	41.0	2,499,609
S3#2*	44.0	48.9	1,211,137
S8#2	51.1	56.7	396,489
S5#1	51.4	57.1	199,956
S6#1 (2)	52.0	57.8	197,275
S6#2 (2)	64.1	70.4	28,371
S9#1	90.0	99.0	17,501

*test stopped at cycle number

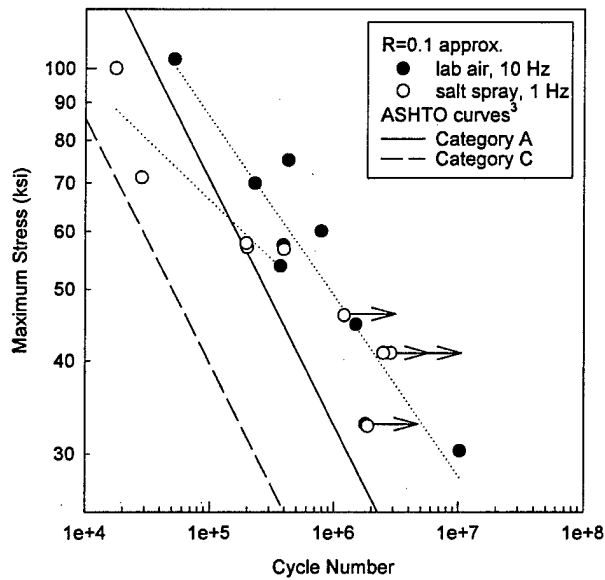


Figure 4 Maximum applied stress versus cycles to failure for weld-repaired AH36 deck sockets tested in three-point bending.

Table V Linear regression results of the fatigue life data using the equation $\log\Delta\sigma = m\log N + b$ or $\log\sigma_{\max} = m\log N + b$.

	m	b	r ²
$\Delta\sigma$, air tests	-0.234 ± 0.036	3.040 ± 0.211	0.858
$\Delta\sigma$, salt spray tests*	-0.163 ± 0.043	2.591 ± 0.214	0.829
$\Delta\sigma$, AASHTO Category A	-0.333	3.467	NA
$\Delta\sigma$, AASHTO Category C	-0.333	3.217	NA
σ_{\max} , air tests	-0.244 ± 0.037	3.155 ± 0.218	0.859
σ_{\max} , salt spray tests*	-0.163 ± 0.043	2.638 ± 0.214	0.830
σ_{\max} , AASHTO Category A	-0.333	3.516	NA
σ_{\max} , AASHTO Category C	-0.333	3.226	NA

* Only failed specimen data were included in the data regression (5 data points vs. 9 for air).
NA=not available



Figure 5 Optical macrograph of typical specimen tested in air showing fracture along weld and base metal interface.

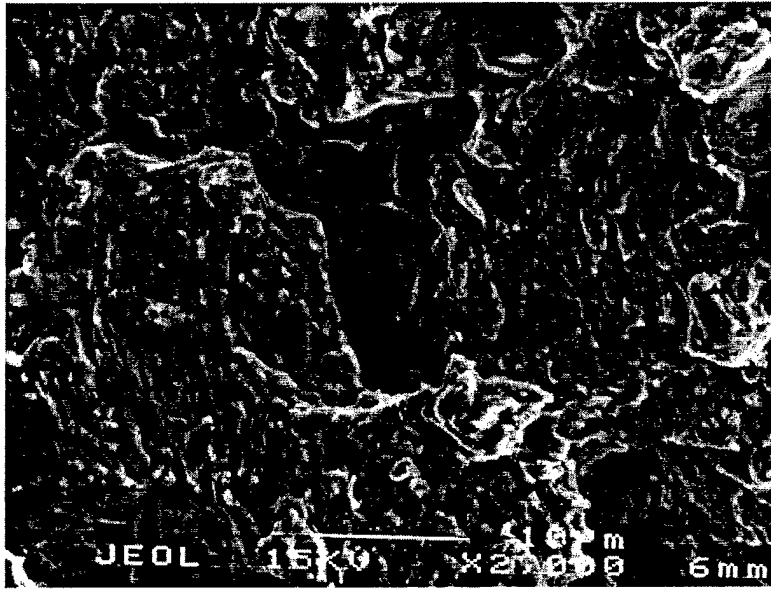


Figure 6 Scanning electron micrograph of specimen S7#1 near fatigue crack tip ($\Delta\sigma=90.4$ ksi= $1.7\sigma_y$, $N_f=51,863$ cycles.)

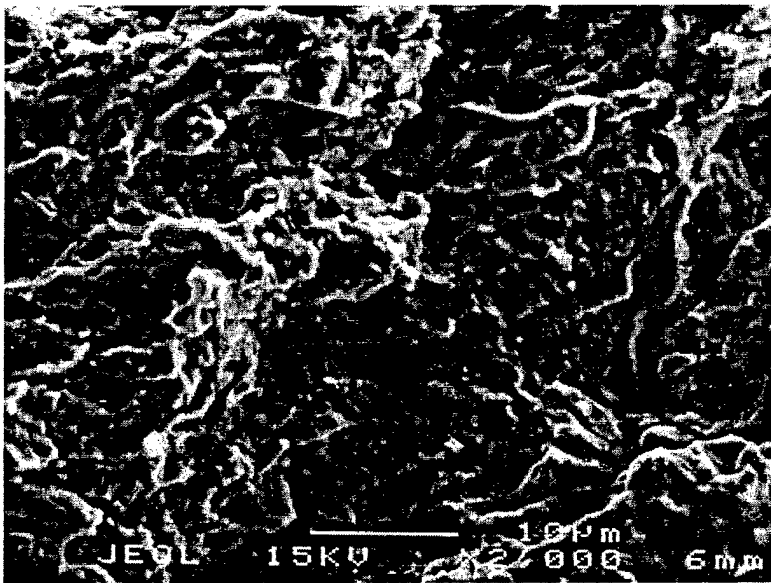


Figure 7 Scanning electron micrograph of specimen S6#2(1) near fatigue crack tip ($\Delta\sigma=30.4$ ksi= $0.6\sigma_y$, $N_f=10,302,827$ cycles.)

fatigue striations (or striation bundles) compared to the specimen tested at a low stress (Fig. 7), as expected.

The salt spray schedule employed resulted in significant corrosion of the specimen surface and was considered to be a relatively severe condition. The fracture surfaces of specimens tested in air were compared to those tested under the salt spray schedule at the same stress levels. No significant differences in fracture mode were observed.

DISCUSSION

Effects of the Salt Spray Schedule on Fatigue Life

The primary goal of this work was to assess the shift in the fatigue initiation curve due to the marine environment. Reduced fatigue strength due to corrosion is usually the result of the simultaneous action of cyclic stress and the environment. Previous work has shown that the fatigue strength of a steel equivalent to ABS EH36 tested in seawater (notched specimen, $k_t=1.3$) is reduced by a factor of 1.3 compared to an identical specimen tested in air at 10^6 cycles⁴. The fatigue reduction factor increases to 2.2 at 10^7 cycles. A smaller effect was also observed in the low cycle regime. Reference [4] showed that the effects of corrosion are more damaging in high cycle than low cycle fatigue.

Figs. 3 and 4 show that there is a negligible effect of the salt spray schedule at the longer fatigue lives that were obtained in this study. This may be due to the irregular contour of the weld and its large effect on the fatigue life. Other studies have shown improved fatigue initiation resistance upon increases in the contact angle between the weld and the basemetal at the toe of the weld⁷ or the removal of the weld reinforcement⁸. The role of this surface in fatigue initiation is shown here by the observed fracture initiation at the weld/base metal interface within the fusion zone. This interface acts as an additional stress concentrator and initiation is aided by the difference in strength between the weld metal and the base metal, as mentioned earlier. It was also observed that the specimens that fractured within the weld possessed large lack of fusion or penetration defects that possessed a larger stress concentration factor than the surface contour at the fusion zone. These results indicate that large surface irregularities have a dominant effect on fatigue life. These results can explain why little effect of corrosion is observed at long lives. If fatigue initiation is controlled by the large surface irregularities of the weld surface, the smaller inhomogeneities introduced by surface corrosion will have little effect on fatigue initiation behavior. In addition, direct comparison the behavior observed in this study to the behavior obtained under full immersion may not be feasible. It is likely that different corrosion fatigue initiation and propagation mechanisms are acting.

Figs. 3 and 4 show that at high stresses and short fatigue lives ($\Delta\sigma=1.2-1.7\sigma_y$), a significant effect of the salt spray schedule was observed. A study discussed previously showed an effect of saltwater immersion on the low cycle fatigue behavior of notched specimens⁴; however, the magnitude of the effect was less than in the high cycle regime.

For example, the fatigue strength reduction factor ($\Delta\sigma_{\text{air}}/\Delta\sigma_{\text{saltwater}}$) decreased from 2.3 to 1 for fatigue lives ranging from 900 to 1×10^5 cycles⁴. It appeared that in this work the notch served to localize the corrosion attack and accelerate fatigue initiation. Specimen examination revealed localized corrosion along the fusion zone in specimens S6#2(2) and S9#1. In contrast, the corrosion observed in the lower stress level specimens was more uniformly distributed on the specimen surface. It is well known that more heavily cold worked regions of a material exhibit higher corrosion rates. Therefore, it is possible that localized corrosion and an accelerated corrosion rate is obtained at regions of high plastic deformation, resulting in shorter fatigue lives compared to tests conducted in air, and a higher fatigue strength reduction than tests conducted at low stress levels. Additional study is required to verify this.

Comparison of Results to AASHTO Curves

In Figs. 3 and 4, Category A refers to the AASHTO S-N curve for a variety of base-metal steels, and Category C refers to the AASHTO S-N curve for a variety of weld-repaired steels. Comparison of the results from this study to the large-scale specimens used to obtain the AASHTO curves warrants some discussion.

Regression of a large amount of fatigue data from multiple sources results in a variety of S-N relations. It was found that this variation is a result of differences in specimen size, with the lower bound established by large-scale specimens⁹. Data obtained from small-scale specimens typically shows a higher apparent fatigue strength and a more positive slope (m) associated with log-log plot of applied stress versus cycles to failure.

The specimen size dependency can be explained by two effects. Fatigue life is controlled by accumulated localized plastic strain at defects. Therefore, a large specimen has a higher probability of containing a surface defect that will initiate a fatigue crack compared to a small specimen, and will result in a lower bound fatigue strength. In addition, this effect becomes more significant at low stress ranges, resulting in a more positive value of the exponent m for small-scale test specimens. Secondly, if testing of weld material is involved, large specimens will contain higher residual stresses than small specimens due to lack of constraint in the small specimens. This is true also for small specimens extracted from large-scale members⁹.

The data in Fig. 3 is consistent with the specimen size dependencies described above. The small-scale specimens removed from the deck sockets do show higher fatigue strengths and a more positive exponent m compared to the large-scale AASHTO specimens. The deck sockets do not contain welds larger than those tested in the small-scale specimens. However, the effect of defect distribution still remains due to the limited number of specimens that were tested. It is possible that we did not sample a specimen with a defect large enough to result in a lower bound value, while there are enough weld-repaired deck sockets present in a ship to result in a high probability that one does exist. In addition, the state of residual stress and constraint in the small-scale

specimens may not be representative of in-service conditions. Since the AASHTO curves represent a lower bound condition, it will be a conservative estimate of the fatigue behavior and is acceptable for use in the fatigue analyses.

CONCLUSIONS

1. No effect of the salt spray schedule was observed within the low stress, high cycle fatigue regime examined here ($\Delta\sigma = 0.6\sigma_y$ to $1.0\sigma_y$, $N_f = 2 \times 10^5$ to 10^7 cycles).
2. An effect of the salt spray schedule was observed within the high stress, low cycle regime ($\Delta\sigma = 1.2\sigma_y$ to $1.7\sigma_y$, $N_f = 2 \times 10^4$ to 4×10^5 cycles) and an approximate maximum fatigue reduction factor of 1.4 was observed.
3. Comparison of the small specimen fatigue data with AASHTO fatigue curve is consistent with the known effect of specimen size on fatigue behavior. This work has verified that the AASHTO fatigue curve obtained from large welded specimens represents a lower bound for the fatigue behavior of weld-repaired deck sockets tested in air, as well as under a corrosive salt spray schedule. Therefore, use of the AASHTO fatigue curves for analysis of weld-repaired deck socket fatigue life is conservative.

REFERENCES

- ¹ X. Zhang and M. Gaudett, "Fracture Mode Study of AH36 Steel Cloverleaf Deck Sockets", NSWCCD-TR-61-98/13, Naval Surface Warfare Center, Carderock Division, West Bethesda, MD, 1998.
- ² P. Keating and J. Fisher, "Evaluation of Fatigue Tests and Design Criteria on Welded Details", National Cooperative Highway Research Program Report No. 286, Transportation Research Board, National Research Council, Washington, D.C., 1986.
- ³ G. Miller and H. Reemsnyder, "Strain-Cycle Fatigue of Sheet and Plate Steels III: Tests of Notched Specimens", SAE Technical Paper Series, 830176, International Congress and Exposition, Detroit Michigan, 1983.
- ⁴ M. Gross and E. Czyryca, "Effects of Notches and Saltwater Corrosion on the Flexural Fatigue Properties of Steels for Hydrospace Vehicles", MEL R&D Report 420/66, U.S. Navy Marine Engineering Laboratory, Annapolis, MD, 1966.
- ⁵ "Standard Practice for Operating Salt Spray (Fog) Apparatus", ASTM B117-97, American Society for Testing and Materials, West Conshohocken, PA, 1997.
- ⁶ Marks' Standard Handbook for Mechanical Engineers, E. Avallone and T. Baumeister eds., McGraw-Hill Inc., New York, NY, 1987, p. 5-6.
- ⁷ K. Richards, "Fatigue Strength of Welded Structures", The Welding Institute, Abington Hall, England, 1969.
- ⁸ B. Kelly and R. Dexter, "Fatigue Performance of Repair Welds", ATLSS Report No. 97-09, ATLSS Engineering Research Center, Lehigh University, Bethlehem, PA, 1997.
- ⁹ "Development of Advanced Double Hull Concepts, Structural Failure Modes: Fatigue", U.S. Navy-Lehigh University Cooperative Agreement N00014-91-CA-001, "Fleet of the Future", TDL-L91-01, Phase I.3a, Vol. 3a, 1993.

INITIAL DISTRIBUTION

Copies		Copies	DIVISION DISTRIBUTION
24	NAVSEA	1	0112 (Douglas)
	1 SEA 03 (Yount)	1	0115 (Messick)
	1 SEA 03M (Kaznoff)	1	27 (Tarasek)
	1 SEA 03M1 (Parks)	1	60 (Wacker)
	1 SEA 03M1 (Brinkerhoff)	1	601 (Morton)
	1 SEA 03M2 (Null)	1	602 (Rockwell)
	1 SEA 03M2 (Dorn)	1	603 (Cavallaro)
	1 SEA 03P (McCarthy)	1	604 (DeSavage)
	1 SEA 03P1 (Packard)	1	605 (Fisch)
	1 SEA 03P1 (Sieve)	1	606 (Conley)
	1 SEA 03P1 (Walz)	1	61 (Holsberg)
	1 SEA 03P2 (Nichols)	1	61s
	1 SEA 03P3 (Schell)	1	62 (Eichinger)
	1 SEA 03P3 (Miles)	1	63 (Alig)
	1 SEA 03P4 (O'Conner)	1	64 (Fischer)
	1 SEA 03P4 (Manuel)	1	65 (Beach)
	1 SEA 03P4 (Moussouros)	1	66 (Riley)
	1 SEA 03U (Leadman)	1	67 (Rockwell)
	1 PMS 385D (Sandison)	1	68 (Mueller)
	1 PMS 350		
	1 PMS 350 (Seawolf Databank)		
	1 PMS 450	1	613 (Ferrara)
	1 PMS 450 (C. Hamilton)	2	614 (Montemarano)
	1 PMS 450 (VA Class Databank)	1	614 (Czyryca)
	1 DSDM Strategic Sealift Design Site (Lynaugh)	10	614 (Gaudett)
		1	614 (Zhang)
3	Office of Naval Research	1	612 (Aprigliano)
	1 1131 (Yoder)	1	615 (Juers)
	1 1131 (Sedriks)	1	653 (Kihl)
	1 332 (Vasudevan)		
		1	3441
1	NRL	1	3442
	1 6310 (Pao)	1	3443
2	DTIC		
1	Naval Post Graduate School		